Available online at www.sciencedirect.com

SciVerse ScienceDirect

Ceramics International 39 (2013) S501–S505

CERAMICS INTERNATIONAL

www.elsevier.com/locate/ceramint

Growth of hexagonal prism ZnO nanorods on Zn substrates by hydrothermal method and their photoluminescence

Nuengruethai Ekthammathat[a], Titipun Thongtem[a,*], Anukorn Phuruangrat[b,**], Somchai Thongtem[c]

[a]Department of Chemistry, Faculty of Science, Chiang Mai University, Chiang Mai 50200, Thailand
[b]Department of Materials Science and Technology, Faculty of Science, Prince of Songkla University, Hat Yai, Songkhla 90112, Thailand
[c]Department of Physics and Materials Science, Faculty of Science, Chiang Mai University, Chiang Mai 50200, Thailand

Available online 16 October 2012

Abstract

Hexagonal prism ZnO nanorods were successfully grown on Zn substrates by the 120 °C and 24 h hydrothermal reaction of the solutions with pH of 9–12. Results from XRD, SEM, TEM, SAED and HRTEM showed that the as-synthesized products were wurtzite ZnO with the shape of hexagonal prism nanorods grown along the [0 0 1] direction with smooth prismatic side planes. The PL spectra showed strong emission band at 543 nm in the green-yellow region due to the recombination of electrons trapped in singly ionized oxygen vacancies and photoexcited holes. This facile, reproducible and effective low-cost approach is promising for the future large-scale synthesis of wurtzite ZnO nanostructures for different applications in nanotechnology.

© 2012 Elsevier Ltd and Techna Group S.r.l. All rights reserved.

Keywords: B. Electron microscopy; B. X-ray methods; D. ZnO; E. Functional applications

1. Introduction

One dimensional (1D) nanostructured materials are usually synthesized by bottom-up directional growth process and are able to be applied in different areas such as transistors, UV light emitters, light emitting diodes, solar cells and gas sensors. Their properties are sensitively influenced by both shape and size, and are of fundamental and technological interests. Thus the development of synthetic method and understanding their formation mechanism are important in nanoscience and nanotechnology [1,2].

Zinc oxide (ZnO) is one of the important semiconductors with 3.37 eV direct band gap at room temperature and large 60 meV exciton binding energy. It is a promising material for efficient emission by low excitation energy at room temperature. Thus ZnO has been recognized as a valuable photonic material in the UV-blue region [1–3]. It is a bio-safe and biocompatible material, and is able to be directly used as a biomedical material with no further coatings [3].

Various methods have been used to synthesize 1D ZnO nanostructures: chemical bath deposition [4], chemical solution [5], sol–gel [6] and chemical vapor deposition (CVD) [7]. However, most of them generally involve two steps: depositing or spin coating of ZnO nanoparticles on substrates to form films of ZnO crystal seeds, and followed by growing of ZnO nanorod arrays on the seed coated substrate in an aqueous solution containing zinc ions [8]. In the present research, hexagonal prism ZnO nanorods were successfully grown on Zn substrates by low temperature hydrothermal reaction. The effect of pH on the formation of hexagonal prism ZnO nanorods on Zn substrates and a possible growth mechanism were proposed and discussed in detail.

2. Experiment

All reagents of this experiment were analytical grade and used without further purification. The hexagonal prism

---

*Corresponding author. Tel.: +66 53 943344; fax: +66 53 892277.
**Corresponding author. Tel.: +66 74 288374; fax: +66 74 288395.
E-mail addresses: ttpthongtem@yahoo.com (T. Thongtem), phuruangrat@hotmail.com (A. Phuruangrat).

0272-8842/$ - see front matter © 2012 Elsevier Ltd and Techna Group S.r.l. All rights reserved.
http://dx.doi.org/10.1016/j.ceramint.2012.10.122

ZnO nanorods were grown on Zn substrates or foils in sequence as follows. Several of $15\times15\times0.25$ mm Zn substrates were carefully cleaned with deionized water and absolute alcohol in an ultrasound bath, respectively. They were put in NaOH aqueous solutions with the pH of 9–12. Each of the solutions and zinc substrates was transferred into Teflon-lined stainless steel autoclaves of 50 ml capacities. The autoclaves were tightly closed, heated at 120 °C in a laboratory electric oven for 24 h, and naturally cooled to room temperature. The zinc substrates were thoroughly washed by deionized water several times, and dried at 70 °C by an electric oven for 12 h for further characterization.

3. Results and discussion

Fig. 1 shows XRD patterns of the as-grown ZnO crystals on Zn substrates synthesized by hydrothermal reaction at 120 °C for 24 h in the solutions with different pH values. Before hydrothermal processing, all diffraction peaks of the substrates could be indexed as pure hexagonal Zn structure of the JCPDS no 04-0831 [9]. Upon hydrothermal processing at 120 °C for 24 h, wurtzite structured ZnO phase of the JCPDS no 36-1451 [9], and those marked with hexagonal Zn of the JCPDS no 04-0831 [9] were detected. It should be noted that the diffraction peaks of the as-synthesized ZnO were strong and sharp, specified as well crystallized products. Preferential orientation of the as-synthesized 1D nanostructured ZnO was determined from peak intensity of the as-synthesized products by comparing with that of the standard bulk. For the as-synthesized ZnO product, intensity of the (0 0 2) peak was higher than that of the (1 0 1) peak. But for the standard bulk ZnO, the (1 0 1) peak is the highest. This could be related to the preferential orientation and alignment of the as-synthesized ZnO crystal on Zn substrate. It was believed that the preferential orientation of ZnO grew along the *c* direction on the Zn substrate [10,11].

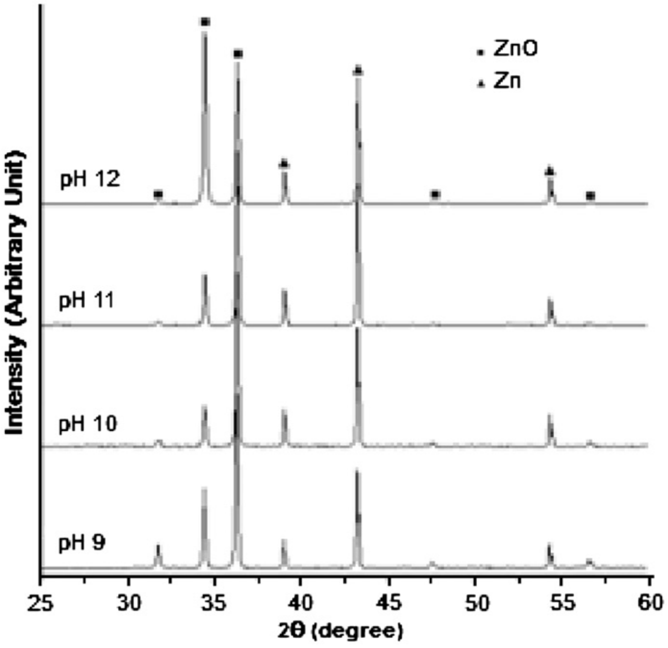

Fig. 1. XRD patterns of ZnO synthesized in the solutions of different pH values by the 120 °C and 24 h hydrothermal reaction.

The extent of *c* orientation of the as-synthesized ZnO crystals was explained by the relative texture coefficient (RTC) [12]. For random crystallographic orientation, RTC of ZnO is 0.5. In this research, RTC at (0 0 2) peak is 0.74, which supported the preferential orientation of the as-synthesized ZnO crystals grew along the [0 0 1] direction on the Zn substrate.

Morphologies of the as-synthesized ZnO products grown on Zn substrates were observed by SEM (Fig. 2). It showed that the product morphologies gradually developed from nanoparticles to nanorods, controlled by the pH of the solution. At pH 9, the surface of the zinc substrate was uniformly covered with ZnO nanoparticles. ZnO nanoparticles began to grow as ZnO nanorods at the pH 10. Upon increasing the pH of the solution to 12, the Zn substrate was densely covered with 1 μm long ZnO nanorods with 100–500 nm in diameters. The high-magnification of SEM image (inserted in Fig. 2d) revealed that ZnO crystals were hexagonal prismatic columns of well-resolved edges and corners with smooth faces. The angles between the two adjacent faces of individual hexagonal nanorods were 120°.

More detail of the product morphologies was investigated by TEM. The general TEM images, HRTEM image and SAED pattern of the as-synthesized ZnO nanorods at the pH 12 are shown in Fig. 3. TEM images show hexagonal columnar ZnO nanostructures with diameter range of 20–80 nm and lengths of several hundred nanometers. The corresponding SAED pattern indicates that each ZnO nanocolumn was single crystal. It can be indexed to be the hexagonal ZnO phase, in accordance with the above XRD analysis. The HRTEM image shows interplanar space of about 0.28 nm, corresponding to the fringe of (1 0 0) ZnO plane, specified as the single crystal with the preferential growth in the [0 0 1] direction. SAED and HRTEM analysis confirmed that hexagonal prism ZnO single crystals grew along the [0 0 1] direction [3,6]. The formation of hexagonal ZnO nanorods was attributed to the difference in growth rate of the prominent crystalline facets with low surface energies during the growth of crystal. The surface energies of different hexagonal ZnO facets of the (0 0 0 1), (10–11), (10–10) planes are -2.8102, -2.1067 and -2.0013 kJ/mol, respectively. Therefore, the growth rates of the ZnO crystals in different planes are in sequence as follows: (0 0 0 1) > (10–11) > (10–10). Growth rate of the (0 0 0 1) plane was the most rapid leading to the sharp tips at the end of the nanorods. Growth rate of the (10–10) plane is at the slowest, and that of the (10–11) plane in the middle; therefore, they remained to form the hexagonal prism ZnO nanorods [8,13,14].

In general, size and shape of the products are controlled by the competition between crystalline nucleation and

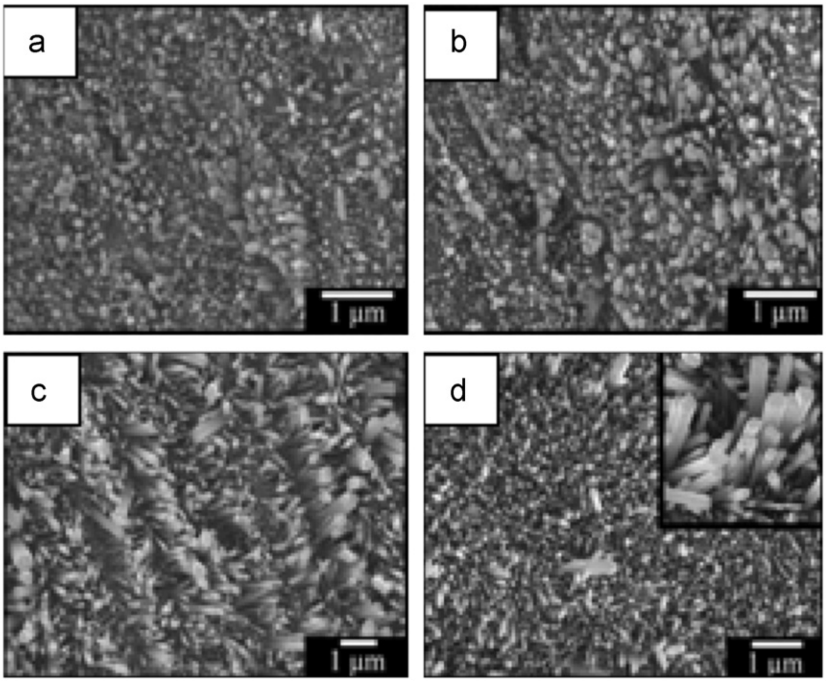

Fig. 2. SEM images of ZnO synthesized in the solutions with the pH of (a–d) 9, 10, 11 and 12 by the 120 °C and 24 h hydrothermal reaction.

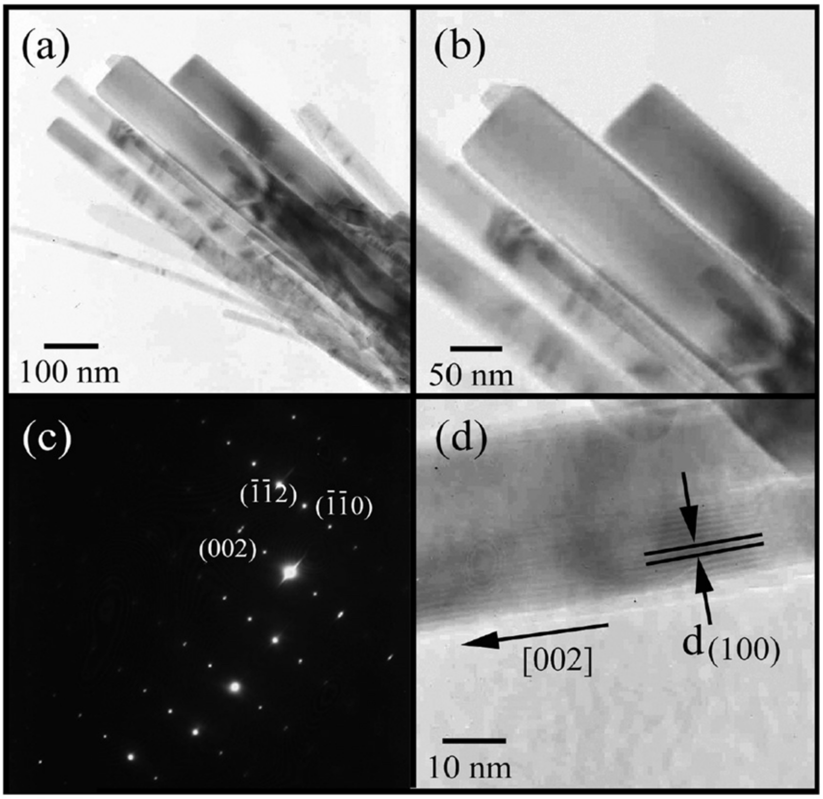

Fig. 3. (a, b) TEM images, (c) SAED pattern, and (d) HRTEM image of hexagonal ZnO nanorods synthesized in the solution with the pH 12 by the 120 °C and 24 h hydrothermal reaction.

growth, determined by the inherent crystal structure and the chemical potential of the precursor solution. For the nucleation rate of more than the growth rate, the crystals are small and low aspect ratio, with a large number of crystals. Contrarily, they are large, high aspect ratio and small number. Although the crystal growth is mainly determined by the intrinsic structure, it is affected by the external conditions such as pH, saturation and temperature.

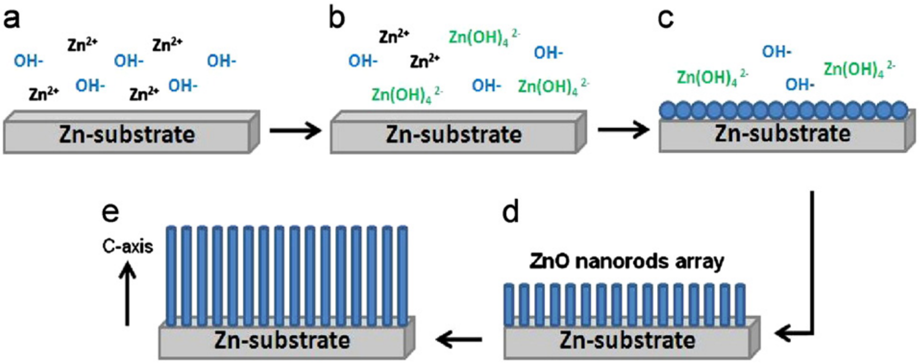

Fig. 4. Schematic diagram of a possible growth mechanism of hexagonal prism ZnO nanorods on Zn substrates.

In this work, pH of the solution was considered to play an important role in the formation of hexagonal prism ZnO nanorods [15,16]. Fig. 4 shows the schematic diagram of a possible growth mechanism of hexagonal prism ZnO nanorods grown on Zn substrate, simply explained in three basic steps. First, Zn substrate was dissolved in basic solution and Zn^{2+} ions formed. Second, $[Zn(OH)_4]^{2-}$ complex ions formed to create multiple nuclei on the zinc substrate. Third, homoepitaxial growth of nuclei proceeded as hexagonal prism ZnO nanorods by the 120 °C and 24 h hydrothermal reaction [8].

By continuously increasing the pH of the solution, a large number of ions were produced. This led the system in forming a supersaturated solution, which favored the formation of hexagonal prism ZnO nanorods. Hence, the facile growth of hexagonal prism ZnO nanorods on Zn substrates was attributed by the alkaline solution with very high concentration of hydroxide anions [8].

The room-temperature PL spectra of hexagonal ZnO (Fig. 5) were measured using 215 nm excitation wavelength. They show the same emission broad band at 510–640 nm with a strong band at 543 nm, corresponding to the green-yellow emission due to the recombination of electrons trapped at singly charged oxygen vacancies and photogenerated holes [17,18]. The emission became weakened by the desorption of OH^- groups on the surfaces of ZnO nanorods.

In general, two emissions were detected on ZnO nanorods: UV range caused by the recombination of electrons in conduction band and holes in valence band relating to band gap, and visible range by surface defects of crystals. Different rationalizations were caused by the change in PL of 1D ZnO nanostructures. The UV emission intensity is the maximum, when the 1D ZnO nanostructures have an orientation along the *c*-axis, and increases as the crystallite size increases. Meanwhile, surface defects, interstitial defects, and the adsorption of impurities on the surfaces of the nanorods can lead to different emissions in the visible range. Among the different defects are oxygen vacancy, zinc vacancy, oxygen interstitial, zinc interstitial and antisite oxygen. Oxygen vacancy is at the most to be mentioned. In general, visible emission is caused by the recombination of electrons trapped in singly charged oxygen vacancies and photogenerated holes. Sometimes the photogenerated holes are first trapped on the product surface, diffused into the bulk, and subsequently combined with electrons trapped at the singly charged oxygen vacancies to form doubly charged oxygen vacancies. The recombination of holes at doubly charged oxygen vacancies and electrons in conduction band leads to the emission of visible spectrum. Considering the green emission, it is known to be the recombination of photogenerated holes with electrons occupying intrinsic defects, such as singly charged oxygen vacancies and antisite oxygen atoms. The emission intensity is increased with the increase in the concentration of defects, including the band bending effect due to the chemisorption of oxygen and the crystal. The yellow emission is caused by the zinc interstitial atoms [19,20].

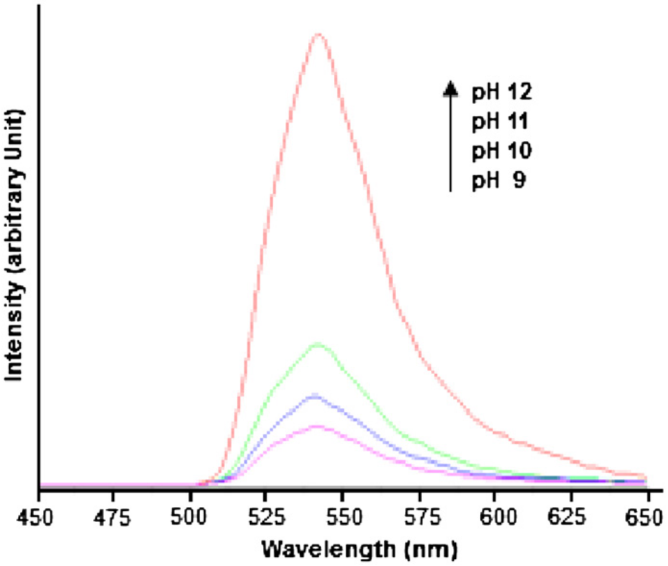

Fig. 5. PL spectra of ZnO synthesized by the 120 °C and 24 h hydrothermal reaction.

4. Conclusions

The good crystalline hexagonal prism ZnO nanorods with high density were synthesized on Zn substrates by the

120 °C and 24 h hydrothermal reaction without the use of any catalysts or additives. Phases of the products were investigated by XRD, specified as wurtzite hexagonal ZnO structure on Zn substrates. SEM and TEM images revealed the presence of the hexagonal prism ZnO nanorods, preferentially grown along the [0 0 1] direction. Room temperature PL spectra were sharp and strong with the green-yellow emission at 543 nm.

Acknowledgments

We wish to thank the Thailand's Office of the Higher Education Commission for providing financial support through the Human Resource Development Project in Science Achievement Scholarship of Thailand, the National Research Council of Thailand through the Research Program for Fiscal Year 2556, and the Graduate School of Chiang Mai University through the general support.

References

[1] S.J. Kim, H.H. Kim, J.B. Kwon, J.G. Lee, B.H. O, S.G. Lee, E.H. Lee, S.G. Park, Novel fabrication of various size ZnO nanorods using hydrothermal method, Microelectronic Engineering 87 (2010) 1534–1536.

[2] T. Ghoshal, S. Kar, J. Ghatak, S. Chaudhuri, ZnO nanocones: Solvothermal synthesis and photoluminescence properties, Materials Research Bulletin 43 (2008) 2228–2238.

[3] A. Umar, S.H. Kim, J.H. Kim, Y.B. Hahn, Structural and optical properties of ZnO nanostructures grown on silicon substrate by thermal evaporation process, Materials Letters 62 (2008) 167–171.

[4] G.Z. Jia, Y.F. Wang, J.H. Yao, Fabrication and strain investigation of ZnO nanorods on Si composing sol-gel and chemical bath deposition method, Journal of Physics and Chemistry of Solids 73 (2012) 495–498.

[5] J. Zhao, Z.G. Jin, T. Li, X.X. Liu, Nucleation and growth of ZnO nanorods on the ZnO-coated seed surface by solution chemical method, Journal of the European Ceramic Society 26 (2006) 2769–2775.

[6] K. Prabakar, H. Kim, Growth control of ZnO nanorod density by sol-gel method, Thin Solid Films 518 (2010) e136–e138.

[7] T. Hirate, S. Sasaki, W. Li, H. Miyashita, T. Kimpara, T. Satoh, Effects of laser-ablated impurity on aligned ZnO nanorods grown by chemical vapor deposition, Thin Solid Films 487 (2005) 35–39.

[8] D. Wang, C. Song, Z. Hu, W. Chen, X. Fu, Growth of ZnO prisms on self-source substrate, Materials Letters 61 (2007) 205–208.

[9] Powder Diffract. File, JCPDS-ICDD, 12 Campus Boulevard, Newtown Square, PA 19073-3273, U.S.A. (2001).

[10] L. Yang, J. Yang, D. Wang, Y. Zhang, Y. Wang, H. Liu, H. Fan, J. Lang, Photoluminescence and Raman analysis of ZnO nanowires deposited on Si(100) via vapor–liquid–solid process, Physica E 40 (2008) 920–923.

[11] Y.J. Gao, W.C. Zhang, X.L. Wu, Y. Xia, G.S. Huang, L.L. Xu, J.C. Shen, G.G. Siu, P.K. Chu, Hydrothermal self-assembling of ZnO nanorods into sphere-like superstructures and their optical characteristics, Applied Surface Science 255 (2008) 1982–1987.

[12] F. Li, Z. Li, F.J. Jin, Structural and luminescent properties of ZnO nanorods prepared from aqueous solution, Materials Letters 61 (2007) 1876–1880.

[13] C.W. Yao, H.P. Wu, M.Y. Ge, L. Yang, Y.W. Zeng, Y.W. Wang, J.Z. Jiang, Triangle-shape ZnO prepared by thermal decomposition, Materials Letters 61 (2007) 3416–3420.

[14] Z. Fang, K. Tang, G. Shen, D. Chen, R. Kong, S. Lei, Self-assembled ZnO 3D flowerlike nanostructures, Materials Letters 60 (2006) 2530–2533.

[15] J.H. Yang, J.H. Zheng, H.J. Zhai, L.L. Yang, J.H. Lang, M. Gao, Growth mechanism and optical properties of ZnO nanosheets by the hydrothermal method on Si substrates, Journal of Alloys and Compounds 481 (2009) 628–631.

[16] W.B. Hu, D.T. Tian, Y.Z. Mi, G.H. Nie, Y.M. Zhao, Z.L. Liu, K.L. Yao, Synthesis and characterization of In_2O_3 nanocube via a solvothermal-calcination route, Materials Chemistry and Physics 118 (2009) 277–280.

[17] H. Zhang, J. Feng, J. Wang, M. Zhang, Preparation of ZnO nanorods through wet chemical method, Materials Letters 61 (2007) 5202–5205.

[18] X. Wang, K. Huo, F. Zhang, Z. Hu, P.K. Chu, H. Tao, Q. Wu, Y. Hu, J. Zhu, Structural regulation and optical properties of one-dimensional ZnO nanomaterials in situ grown from and on brass substrates, Journal of Physical Chemistry C 113 (2009) 170–173.

[19] J. Lee, J. Chung, S. Lim, Improvement of optical properties of post-annealed ZnO nanorods, Physica E 42 (2010) 2143–2146.

[20] L. Zhang, L. Yin, C. Wang, N. Lun, Y. Qi, D. Xiang, Origin of visible photoluminescence of ZnO quantum dots: Defect-dependent and size-dependent, Journal of Physical Chemistry C 114 (2010) 9651–9658.